

Highly fluorescent complexes with 3-isocyanoperylene and *N*-(2,5-di-*tert*-butylphenyl)-9-isocyano-perylene-3,4-dicarboximide[†]

Cite this: DOI: 10.1039/x0xx00000x

Received 00th January 2012,
Accepted 00th January 2012

DOI: 10.1039/x0xx00000x

www.rsc.org/

S. Lentijo,^a J. E. Expósito,^a G. Aullón,^b J. A. Miguel,^{a,*} and P. Espinet^{a,*}

The perylene derivatives 3-isocyanoperylene (Per–N≡C) (**4a**) and *N*-(2,5-di-*tert*-butylphenyl)-9-isocyano-perylene-3,4-dicarboximide (PMI–N≡C) (**4b**) were prepared and used to synthesize gold complexes [AuX(CNR)] (X = C₆F₅ (**5a,b**), C₆F₄-O^{*n*}Bu-*p* (**6b**)). The reaction of **5b** and **6b** with HNEt₂ led the carbene complexes [AuX{C(NEt₂)(NHR)}] (**7b**, **8b**), respectively. The molecular structure of complexes **7b**, **8b** have been determined by X-ray diffraction analysis showing intermolecular π–stacking of the perylene groups and C₆F₅ rings, and no Au...Au interactions. The derivative compounds [M(CO)₅(CNR)] (M = Cr (**9a,b**), Mo (**10a,b**) or W (**11a,b**)) and *trans*-[Pd(CNR)₂(C₆F₃Cl₂)₂] (**12a,b**) were also prepared. All complexes exhibit fluorescence associated to the perylene fragment with emission quantum yields, in solution at room temperature, in the range 0.05 – 0.93 and emission lifetimes ~ 4 ns. DFT calculations were performed of the absorption spectra of the ligands Per–N≡C and PMI–N≡C, and representative complexes [Au(C₆F₅)(CNR)], [Cr(CO)₅(CNR)], showing a perylene-dominated intraligand π–π* emissive state, from the HOMO and LUMO orbitals of the perylene chromophore, but with significantly different absorption maxima by influence of the metal fragment, particularly significant in the Per–N≡C derivatives.

Introduction

Perylene derivatives, particularly perylene-3,4:9,10-bis(dicarboximide) (PDI), are organic chromophores with excellent chemical and photochemical stability, high molar absorptivity of visible light, and high fluorescence quantum yield. Their electronic and optical properties can be significantly modified by variation of the substituents in the bay region (1, 6, 7 and 12 positions of perylene diimide unit) and/or in the N atoms of the diimide.^{1,2} Due to these remarkable properties, PDIs are materials that, in addition to their use as industrial important pigments,³ have been utilized or explored in other various optical and electronic applications,^{4,5,6,7,8} or for liquid crystals,⁹ and for highly fluorescent J-aggregates.¹⁰ Also, the incorporation of metal centers to PDI structures at the imide region or at bay positions offers the possibility to modify the photochemistry and photophysics, and as a result their potential applications.¹¹

We have published platinum organometallic complexes of perylene and perylene monoimide (*N*-(2,5-di-*tert*-butylphenyl)perylene-3,4-dicarboximide, PMI) with Pt σ-bonded directly to the perylene core,¹² and have found that, in spite of the fact that attaching directly metal centers to aromatic cores of organic chromophores is usually very detrimental, the coordination of Pt has only a moderate quenching effect on the fluorescence (our organoplatinum derivatives kept 70-80% of the fluorescence intensity of the mother organic molecule).^{13,14} Similar high fluorescence quantum yields have been reported when Pd(II) is directly attached to the PDI core.¹⁵ In contrast, the imine 3-perylenylmetilen-4'-ethyl-aniline and their cyclopalladated complexes have moderate quantum yields (in the range 0.04 – 0.13).¹⁶

The desired high fluorescence properties have also been found for perylene substituted organotrialkynyltin compounds, where an alkyl chain is connecting the perylene core with a trialkynylstannyl group,

thus insulating the fluorophore from the metal;¹⁷ for gold, palladium or platinum attached to perylene through a tetrafluorophenyl linker, because the π systems of the perylene and tetrafluorophenyl fragments are uncoupled;¹⁸ for perylene bisimide metal complexes (with a 4-pyridine unit connecting the bisimide with Pd(II) or Pt(II) diphosphine complex);¹⁹ or for complexes with PDI–terpyridine.²⁰

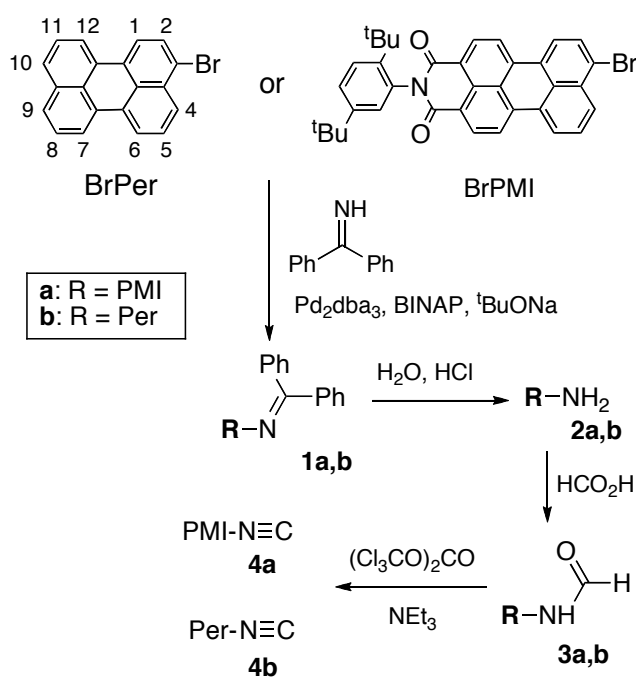
In contrast, for Pt(II) complexes ligated via an acetylide bridge in the bay region to perylenediimide moieties, the fluorescence is quantitatively quenched with production of the ³PDI excite state.²¹ The intense fluorescence of diazadibenzoperylene (Φ_f = 0.80) is also strongly quenched upon metal coordination.²² Also, Cu and Fe metal centers coordinated to a tetramine ligand attached to the PDI core quench its fluorescence.²³

Based on our previous experience on perylene derivatives and luminescent gold complexes containing isocyanide or carbene ligands,^{24,25,26,27} we decided to functionalize perylene and PMI with this coordinating function, which is a fairly general and strong coordinating group for many metals.²⁸ The new ligands should offer a good opportunity to extend this family of derivatives and study the influence of introducing the isocyanide group as connector between a transition metal and the perylene chromophore. We report here the synthesis of 3-isocyanoperylene (Per–N≡C) and *N*-(2,5-di-*tert*-butylphenyl)-9-isocyano-perylene-3,4-dicarboximide (PMI–N≡C). Our initial choice of PMI–N≡C was meant to improve the solubility of the metal derivatives, but soon it was realized that the solubility is similar or even higher for Per–N≡C derivatives than for PMI derivatives and this offered an interesting synthetic simplification for further studies. Au(I), Cr(0), Mo(0), W(0) and Pd(II) complexes with the perylenyl isocyanide ligands have been prepared. The study of the photophysical properties of gold isocyanides has been extended to their respective gold carbenes, which are more soluble derivatives easily obtained by nucleophilic attack with NHEt₂ to the gold-coordinated isocyanide.

Results and discussion

Synthesis of the isocyanide ligands

The syntheses of *N*-(2,5-di-*tert*-butylphenyl)-9-isocyano-perylene-3,4-dicarboximide (**4a**) and 3-isocyanoperylene (**4b**) are outlined in Scheme 1. Following a literature procedure,²⁹ the reaction between *N*-(2,5-di-*tert*-butylphenyl)-9-bromo-perylene-3,4-dicarboximide or 3-bromoperylene with benzophenone imine and a palladium catalyst resulted in the isolation of the ketimines **1a,b**. Hydrolysis of **1a,b** with a catalytic amount of HCl in wet THF gave 9-amino-*N*-(2,5-di-*tert*-butylphenyl)-perylene-3,4-dicarboximide (**2a**) or 3-aminoperylene (**2b**) respectively, which were heated with formic acid in refluxing toluene to prepare the corresponding formanilides (**3a,b**). Finally, dehydration of **3a,b** with bis(trichloromethyl)carbonate (triphosgene) in CH₂Cl₂,^{30,31} yielded **4a,b** in moderate yield (>50%). At room temperature, these isocyanides are red-brown (**4a**) or yellow-brown (**4b**) solids, not particularly odoriferous, that can be stored for long periods in the freezer and show a similar solubility in solvents commonly used.



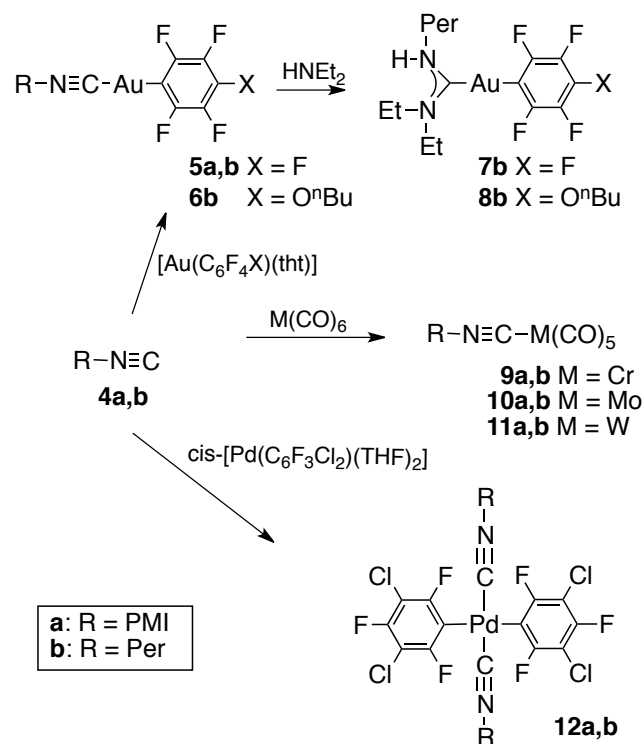
Scheme 1 Synthesis of the isocyanide ligands

One $\nu(\text{C}\equiv\text{N})$ IR absorption is observed, at 2112 cm^{-1} for PMI-N $\equiv\text{C}$ (**4a**) and at 2120 cm^{-1} for Per-N $\equiv\text{C}$ (**4b**). The IR spectrum of PMI-N $\equiv\text{C}$ show additionally the expected $\nu(\text{C}=\text{O})$ absorptions, at 1708 and 1664 cm^{-1} .

Gold complexes. The gold(I) compounds [AuX(CNR)] (**5a,b-6b**) were easily prepared in good yield, as orange solids, by 1:1 reaction of [AuX(tht)] (tht = tetrahydrothiophene, X = C₆F₅, C₆F₄-OⁿBu-*p*) with the corresponding perylene-isocyanide (Scheme 2), in CH₂Cl₂.

The elemental analyses, yields, relevant IR data, and ¹H and ¹⁹F NMR data for the complexes are given in the Experimental section. The IR spectra of **5a,b** and **6b** show one $\nu(\text{C}\equiv\text{N})$ absorption *ca.* 2201 cm^{-1} . This is about 90 or 80 cm^{-1} higher than for the free isocyanide, as an effect of coordination to gold(I).^{27,32} The PMI derivative **5a** is

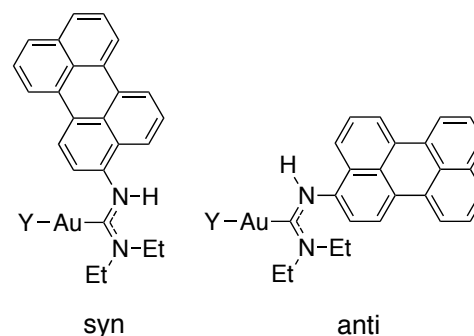
only sparingly soluble and could not be characterized in solution by NMR. For the same reason it could not be further elaborated to produce other derivatives. The ¹H NMR in THF-*d*₈ of **5b** and **6b** are very similar in the aromatic region and differ in the aliphatic region of the spectrum, where **6b** shows the signals of the group OⁿBu.



Scheme 2 Synthesis of the isocyanide complexes

Taking advantage of the known reactivity of coordinated isocyanides towards nucleophiles,^{33,34} we have prepared neutral gold carbenes **7b** and **8b** by nucleophilic attack with a secondary amine (NH_{Et}) to the gold-coordinated isocyanide in [AuX(CN-Per)] (**5b-6b**). The solubility of the two carbenes in organic solvents is higher than for the corresponding gold isocyanides complexes.

Chart 1



The IR spectra of the gold carbene complexes show the disappearance of the $\nu(\text{C}\equiv\text{N})$ absorption and the appearance of new peaks corresponding to $\nu(\text{N}-\text{H})$ and $\nu(\text{C}=\text{N})$ at *ca.* 3353 cm^{-1} and at 1542 cm^{-1} , respectively.^{26,35} For secondary amines with identical

substituents, such as Et₂NH, assuming easy rotation of the perylene ring but severe restriction to rotation about the carbene C–N bond (which has considerable multiple character), only two isomers are possible, syn and anti depending on the arrangement of the perylene group relative to the gold (Chart 1). The ¹H and ¹⁹F NMR spectra in THF-d₈ for **7b** and CDCl₃ for **8b** displayed only one set of ¹H or ¹⁹F resonances indicating the formation of one isomer. A NOE effect with the methylene of one of the ethyl group (at higher field) of the carbene supports the less hindered isomer syn. The observed isomer shows the N–H signal at 9.28 ppm, for **7b** and at 7.72 ppm for **8b**. The ¹H NMR spectra of **7b** and **8b** displayed two signals from the nonequivalent CH₂ of the NEt₂ group (at 4.19 and 3.71 ppm) and two overlapped triplets at 1.43 ppm. As expected, the ¹⁹F NMR spectrum of **7b** displayed the characteristic AA'MXX' signals for C₆F₅ (three multiplet resonances at -115.3 (F_{ortho}), -162.4 (F_{meta}), and -162.7 (F_{para}) ppm), whereas **8b** shows two complex multiplets corresponding to an AA'XX' spin system (at -118.1 (F_{ortho}) and -158.1 (F_{meta}) ppm).

Crystal Structures. X-ray quality crystals could be obtained for the complexes **7b** and **8b**. Their molecular structures were determined by single-crystal X-ray diffraction methods and are shown in Fig. 1. Selected bond lengths and angles are given in Table 1. Data collection and refinement parameters are listed in the Experimental Section.

Table 1 Selected interatomic distances (Å) and angles (°) for the complexes **7b** and **8b**.

	7b	8b
Au(1)–C(21)	2.037(5)	2.045(10)
Au(1)–C(40)	2.046(5)	2.050(9)
C(21)–N(2)	1.340(6)	1.316(12)
C(21)–N(1)	1.341(6)	1.329(12)
N(1)–C(1)	1.429(6)	1.437(12)
C(41)–C(40)–C(45)	114.0(5)	113.4(9)
C(21)–Au(1)–C(40)	176.82(18)	177.8(4)
N(2)–C(21)–N(1)	117.3(4)	116.7(9)
N(2)–C(21)–Au(1)	122.6(4)	122.9(8)
N(1)–C(21)–Au(1)	119.9(3)	120.4(7)
C(21)–N(1)–C(1)	123.1(4)	125.3(8)
C(41)–C(40)–C(45)	114.0(5)	113.3(10)

As expected, the complexes show a roughly linear geometry for gold (angle *ca.* 177°). In both cases, the isomer found has the perylene group oriented away from the ethyl groups of the amine. The Au–C_{carbene} and Au–C_{aryl} distances [2.037(5) – 2.050(9) Å] are very close, in perfect agreement with other pentafluorophenylgold(I) carbenes.²⁶ The Au–C_{carbene} bond is slightly longer than in similar acyclic aminocarbenes with Au–Cl (about 2.00 Å), showing the stronger trans-effect of the pentafluorophenyl group as compared with Cl.^{26,36,37}

The C(21)–N(1) and C(21)–N(2) distances (in the range 1.31 – 1.34 Å), are similar to other Au(I) carbene complexes, and shorter than the C(1)–N(1) single bond distances (*ca.* 1.43 Å), indicating considerable π bonding between carbene C and N atoms. The C–C–C angles at the ipso carbon of the C₆F₄ group in both complexes, are less than 120° (114.0(5) for **7b** and 113.3(10)° for **8b**), a typical

feature due to electronic effects of the electropositive metal and the electronegative fluorine substituents at the ortho positions.^{26,38}

In both complexes the perylene fragment is nearly planar but it is arranged with different angles with carbene plane N(1)–C(21)–N(2) (the dihedral angles are 63.02° for **7b**, and 41.75° for **8b**). The shortest Au–Au intermolecular distance between two metallic centers is 6.002 Å for **7b** and 7.085 Å for **8b**, which clearly excludes any Au⋯Au interaction. However there are significant p–p interactions between the aromatic fragments (Figure 2). The plane-to-plane stacking distance of two perylene rings is 3.55 Å for **7b**, and 3.49 Å for **8b**. Moreover, **7b** shows intermolecular π–π stacking of C₆F₅ rings at 3.37 Å distance.

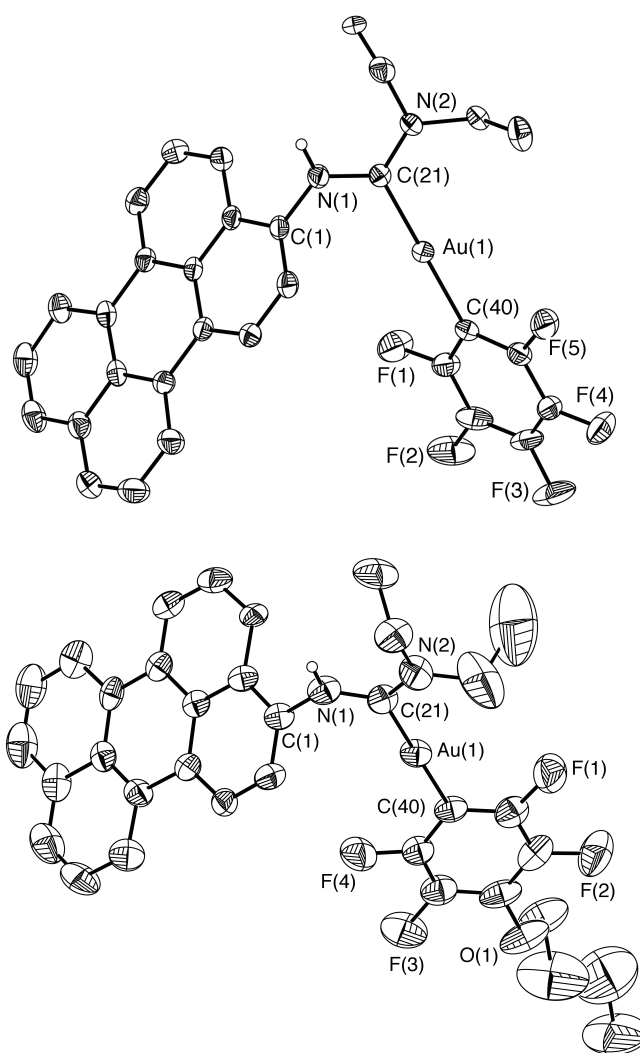


Fig. 1 ORTEP of the crystal structures of **7b** (top) and **8b** (bottom). The ellipsoids are shown at 30% probability (H atoms are omitted for clarity).

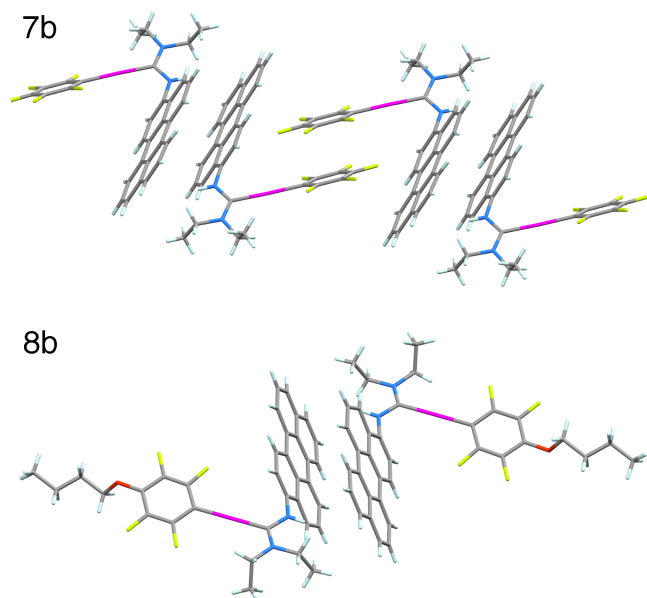


Fig. 2 X-ray packing view of complex **7b** and **8b** showing intermolecular π -stacking of the perylene groups and C_6F_5 rings.

Cr, Mo and W complexes. In order to increase the solubility of metal derivatives with the isocyanide ligands, and test the changes of the optical properties compared to other metal centers, we synthesized the rather soluble complexes $[M(CO)_5(C\equiv N-R)]$ with $M = Cr, Mo, W$. $[Cr(CO)_5(C\equiv N-R)]$ (**9a,b**) were obtained by reaction of the corresponding isocyanides **4a,b** with $[Cr(CO)_5(NCMe)]$, prepared “in situ” from $Cr(CO)_6$ and Me_3NO in acetonitrile.³⁹ The complexes $[M(CO)_5(C\equiv N-PMI)]$ ($M = Mo$, **10a**; W , **11a**) were prepared by reacting the corresponding metal carbonyls with Me_3NO and the isocyanide **4a** in THF, leading to the formation of a reddish-brown compound. The IR spectra of the $[M(CO)_5(C\equiv N-R)]$ complexes display one $\nu(C\equiv N)$ band at *ca.* 2127 cm^{-1} for **9a-11a** and at *ca.* 2131 cm^{-1} for **9b-11b**, at wavenumbers about 15 cm^{-1} , higher than for the free isocyanide (2112 cm^{-1} for **4a**; 2120 cm^{-1} for **4b**) but clearly lower than in the gold complexes **5a,b** (*ca.* 2200 cm^{-1}), showing that gold metal complex fragments are stronger electron acceptors than the metal carbonyl moiety of $M(CO)_5$ as a consequence of coordination.⁴⁰ The IR spectra also show three $\nu(C=O)$ absorptions characteristic for their octahedral structure. The 1H NMR spectra in $CDCl_3$ of **9a,b**, **10a,b** and **11a,b** are similar with some signals slightly deshielded ($< 0.1\text{ ppm}$) from their position in the free isocyanide.

Palladium complexes. The reactions of $PMI-N\equiv C$ or $Per-N\equiv C$ with $[cis-(C_6F_3Cl_2)_2Pd(THF)_2]$ in dichloromethane at room temperature, afford respectively red and yellow complexes $[(C_6F_3Cl_2)_2Pd(CN-R)_2]$ **12a,b**. Their IR spectra show only one $\nu(C\equiv N)$ absorption (2170 cm^{-1} for **12a** and 2176 cm^{-1} for **12b**) for the isocyanide groups, at higher wavenumbers (*ca.* 60 cm^{-1}) than for the free isocyanide, as reported for other palladium(II) isocyanide compounds.^{21,41} This indicates a *trans* arrangement of the two isocyanides (D_{2h} symmetry),⁴² probably preferred to minimize the steric hindrance between the two bulky isocyanide groups.

Complex **12b** is insoluble in common organic solvents and could not be characterized by NMR, not even by optical spectroscopy. The higher solubility of **12a** allows the recording of the 1H and ^{19}F NMR spectra in $THF-d_8$ and, as expected, the data confirm the presence of only one isomer.

Photophysical Studies

(a) UV-Vis absorption spectra. The absorption spectra of the precursors PMI, perylene, the isocyanides $PMI-N\equiv C$ (**4a**) y $Per-N\equiv C$ (**4b**), and their complexes are shown in Figure 3 (only one representative complex of each family is plotted to facilitate observation (Fig. S1 and S2 in ESI show the spectra of all the compounds). Quantitative data for all the compounds are summarized in Table 2.

The profiles of the UV-Vis absorptions of $PMI-N\equiv C$ (**4a**), $Per-N\equiv C$ (**4b**), and their related complexes **1-8** are very similar, and they are dominated by the $\pi-\pi^*$ transition of the perylene moiety (see Fig. 3). The absorption spectra consist of a strong absorption at *ca.* 250 nm , with a more or less defined shoulder, and one band (at $360-460\text{ nm}$ for perylene derivatives and $400-570\text{ nm}$ for PMI derivatives) that resemble the spectrum of perylene or PMI, respectively. These lowest energy bands have a vibronic structure with a vibrational spacing of $\sim 1300\text{ cm}^{-1}$, related to the $\nu(C=C)$ frequency of the polyaromatic system.

Table 2. UV-Vis absorption of $PMI-N\equiv C$ (**4a**), $Per-N\equiv C$ (**4b**) and their complexes in chloroform at 298 K .

Comp	λ , nm ($\epsilon/10^3\text{ M}^{-1}\text{ cm}^{-1}$)
1a	273 (158.1), 356 (5.3), 535 (41.5)
2a	277 (75.6), 358 (6.1), 377 (5.5), 562 (34.3)
3a	264 (105.1), 270 (101.6), 341 (3.1), 357 (3.4), 508 (3.5)
4a	240 (32.9), 255 (29.1), 263 (45.0), 341 (4.9), 450 (20.7), 478 (39.7), 507 (44.8)
1b	260 (58.2), 441 (25.8), 465 (31.1)
2b	261 (25.1), 340 (1.5), 448 (14.7)
3b	258 (36.4), 397 (11.2), 423 (26.5), 448 (32.1)
4b	259 (36.6), 344 (4.5), 402 (11.6), 427 (27.1), 453 (35.7)
5a	264 (156.2), 359 (4.7), 450 (19.9), 476 (43.1), 508 (57.1)
9a	237 (52.2), 264 (42.1), 296s (14.4), 358 (4.3), 469s (16.0) 504 (31.7), 533 (37.6)
10a	239 (101.54), 264 (60.0), 295s (22.0), 357 (6.2), 467s (20.9), 501 (43.7), 532 (54.0)
11a	237 (69.4), 265 (38.9), 265 (38.9), 357 (4.9), 465s (13.3), 502 (30.1), 534 (37.3)
12a	245 (102.1), 255 (106.1), 263 (123.2), 341 (10.1), 359 (8.5), 450 (40.4), 478 (86.9), 511 (114.6)
5b	240 (41.6), 262 (60.7), 346 (3.4) 420 (18.3), 444 (34.6), 471 (43.2)
6b	262 (53.5), 346 (1.2), 420 (17.3), 444 (34.9), 471 (43.5)
7b	256 (38.7), 398 (11.2), 424 (27.8), 450 (33.9)
8b	256 (40.1), 398 (11.2), 424 (27.1), 450 (32.9)
9b	262 (64.1), 420 (18.4), 444 (39.4), 473 (52.4)
10b	247 (73.5), 422 (18.2), 445 (37.6), 474 (48.5)
11b	242 (89.4), 423 (19.1), 444 (44.0), 476 (60.7)

The introduction of the isocyanide group ($-N\equiv C$) perturbs weakly the electronic spectrum of PMI and leads to a more defined vibronic structure than PMI. In fact, the relative peak intensity and the vibronic structure becomes more similar to that of perylene, with increasing intensity of the vibronic bands as we move to higher λ values. The visible absorption spectrum of $Per-N\equiv C$ is similar to that of perylene, but showing a less defined vibronic structure. Since the vibrational fine structure is reduced when the aromatic residue is involved in more extensive conjugation,⁴³ this suggests that the

isocyanide group slightly decreases the conjugation in the PMI but increases it in the perylene. This effect can be nicely observed in the shapes of the LUMO functions for PMI-H and PMI-NC (see the zone highlighted by an arrow in Fig. 4; see below, molecular orbital calculations), where the lobal distribution is more dissimilar for PMI-NC than for PMI-H.

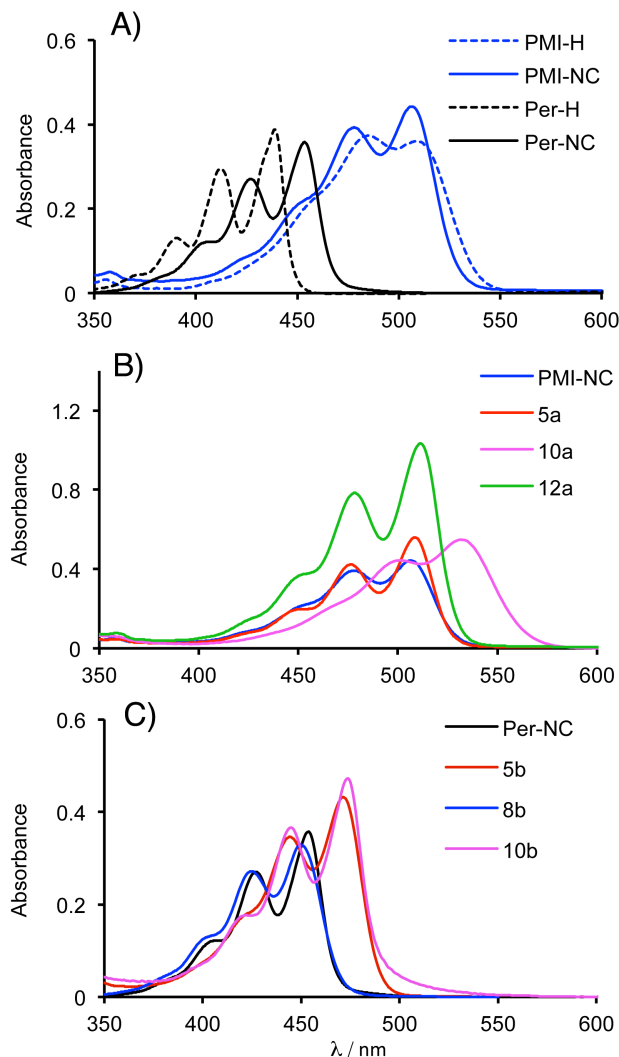


Fig. 3 Absorption spectra recorded in CHCl_3 solution ($\sim 10^{-5}$ M) at room temperature: A) PMI-N \equiv C (**4a**), Per-N \equiv C (**4b**) and their precursors PMI-H and perylene; B) PMI-N \equiv C (**4a**) and their complexes **5a**, **10a**, and **12a**; C) Per-N \equiv C (**4b**) and their complexes **5b**, **8b**, and **10b**.

The lowest energy band for PMI-N \equiv C is blue-shifted about 200 cm^{-1} , compared to PMI, and a red-shifted of 700 cm^{-1} is observed for Per-N \equiv C relative to perylene. The redshifts (relative to the respective free isocyanide) of **5a** and **5b** (40 and 840 cm^{-1} respectively) show a different influence of the AuC_6F_5 on the electronic absorption energies depending on the isocyanide substituent. Larger bathochromic shifts are observed for Per complexes, in contrast with previous observations on related complexes.¹² The shifts to higher wavelength observed by coordination to the $\text{M}(\text{CO})_5$ group (complexes **9a-11a** and **9b-11b**) are very similar (*ca.* 1000 cm^{-1}) regardless of the metal.

The perturbation by interaction of the carbene group with the perylene orbitals is quite different from that produced by isocyanide

group. Thus, the absorption maxima in carbene complexes **7b** and **8b** appear at 450 nm , blue shifted (990 cm^{-1}) from gold isocyanide complexes **5b** and **6b**, and red shifted only 550 cm^{-1} from perylene.

Molecular orbital calculations

DFT calculations were performed on representative perylene derivatives in order to assign the orbitals involved in the electronic transitions observed in the absorption spectra. The selected molecular species PMI-H, Per-H, PMI-N \equiv C (**4a**) and Per-N \equiv C (**4b**), and the complexes $[\text{Cr}(\text{CO})_5(\text{CNR})]$ (**9a,b**) and $[\text{Au}(\text{C}_6\text{F}_5)(\text{CNR})]$ were calculated.

For PMI-H and Per-H the perylene units are planar, and the carbon-carbon lengths suggest the presence of two naphthalenyl entities connected by C-C distances 1.47 \AA . Other internal C-C distances for the fused ring are 1.43 \AA whereas external ones are less than 1.41 \AA . This analysis agrees with experimental data from Cambridge Structural Database.⁴⁴ The conjugate diimido fragment in PMI shows C-O and C-N distances of 1.22 and 1.41 \AA , respectively, and the aryl group of the 2,5-di-*tert*-butylphenyl substituent is practically perpendicular to the perylene structure. These motifs are kept in the all the compounds studied in this work.

The absorption spectra were calculated by TD-DFT, in gas phase and in chloroform. In all cases, the solvent effect of chloroform produces an additional red shift of the absorption, also in the complexes, increasing the wavelength up to 30 nm . Fig. 4 displays a correlation diagram showing the energy and the atomic orbital composition of the HOMOs and LUMOs of perylene, PMI-H, their isocyanide derivatives **4a,b** and the complexes **5a,b** and **9a,b**. These MOs provide the framework for the description of the excited states that govern the absorption and emission processes in these compounds.

For perylene, two bands at 442 and 257 nm are predicted in chloroform solution (experimentally at 439 and 254 nm) and 428 and 253 nm in gas phase, corresponding to transition between the π orbitals. The first peak is the less intense ($f \approx 0.48$), and it corresponds to the HOMO \rightarrow LUMO transition. The second band ($f \approx 0.51$) is assigned to a combination of several transitions between π orbitals of the perylene. The major contribution is a transition between the HOMO and higher empty MO, plus a smaller contribution by a transition between a lower occupied MO and the LUMO (the four orbitals are shown in Fig. S3 in ESI). Analogously, these bands are also found in the related PMI-H analog system, at 500 and 262 nm in solution (experimentally 512 and 264 nm), and 477 and 260 nm in gas phase, which are red shifted by the effect of the imido group and have an increase of the intensity for the former band ($f \approx 0.77$).

Table 3. Absorption parameters ($\pi_{\text{HOMO}} \rightarrow \pi^*_{\text{LUMO}}$ transition) as wavelengths (λ in nm) and intensities (f) for PMI-H, Per-H, PMI-N \equiv C, Per-N \equiv C, and the complexes $[\text{Cr}(\text{CO})_5(\text{CNR})]$ and $[\text{Au}(\text{C}_6\text{F}_5)(\text{CNR})]$.^a

X	PMI-X		Per-X	
	Gas phase	CHCl_3	Gas phase	CHCl_3
H	477 (0.61)	500 (0.77)	428 (0.36)	442 (0.48)
NC	490 (0.69)	512 (0.86)	446 (0.44)	465 (0.58)
$\text{Au}(\text{C}_6\text{F}_5)$	519 (0.79)	527 (1.08)	474 (0.69)	493 (0.79)
$\text{Cr}(\text{CO})_5$	518 (0.97)	536 (1.14)	468 (0.70)	482 (0.84)

^a A complete assignment of the absorption spectra parameters is available from ESI.

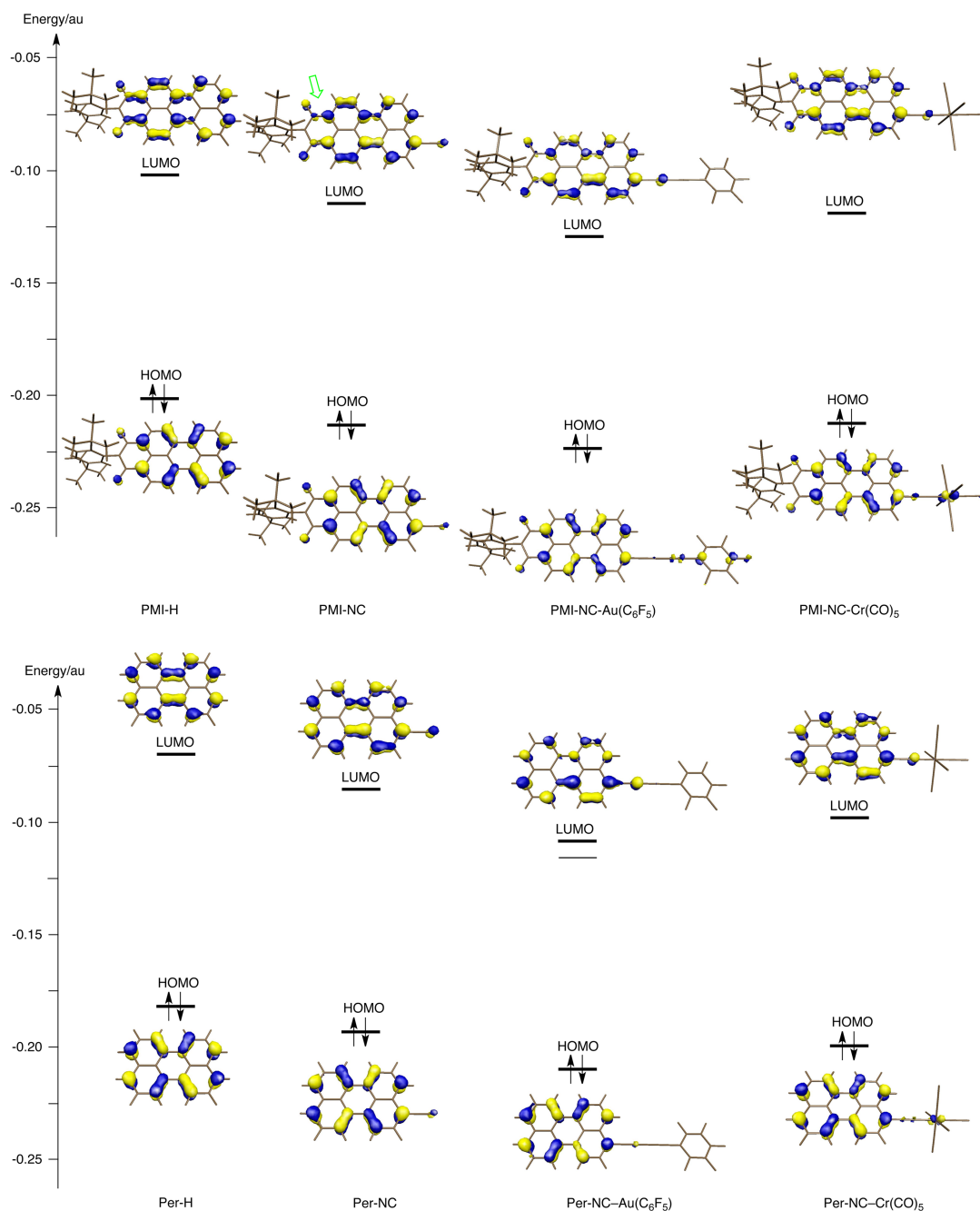


Fig. 4 Orbital contours of the HOMOs and LUMOs for PMI-H, Per-H, PMI-N≡C (**4a**), Per-N≡C (**4b**), and the complexes [Au(C₆F₅)(CNR)] (**5a,b**) and [Cr(CO)₅(CNR)] (**9a,b**) (values HOMO→LUMO transitions are in Table 3).

In the organic compounds PMI-N≡C (**4a**) and Per-N≡C (**4b**) (Table 3 and Fig. 4) the π orbital (of the isocyanide) is close in energy to the π system of the perylene or PMI-H, interact with the aromatic systems and consequently produces a red shift decreasing the energy gap between the involved orbitals and increase the wavelength. Numerically, the predicted first absorption is located at

512 nm ($f \approx 0.86$) for **4a** and 465 nm ($f \approx 0.58$) for **4b** (the experimental values are 507 and 456 nm, respectively). A second band, at 263 ($f \approx 0.22$) for **4a** and 260 nm ($f \approx 0.44$) for **4b** (experimentally at 263 and 259 nm), has a lower intensity than the former, and is assigned to a combination of several transitions between p orbitals of the perylene group.

The lower energy absorptions for PMI-NC-Au(C₆F₅) (**5a**) and PerNC-Au(C₆F₅) (**5b**) correspond to the HOMO → LUMO transition and are calculated to appear at 527 and 493 nm. This is in good concordance with the experimental values of 508 and 471 nm, respectively, and the calculated red shifts, much lower for the PMI derivative and close to its free ligand, are reasonably well reproduced (calculated red shifts for **5a** and **5b**: 556 and 1221 cm⁻¹; experimental red shifts: 154 and 844 cm⁻¹). The calculations with the fragment Cr(CO)₅, complexes **9a** and **9b**, predict absorptions in chloroform at 536 and 482 nm, respectively, in good agreement with the experimental values of 533 and 473 nm; for this fragment, red shifts similar to the free isocyanide (ca. 950 cm⁻¹) are predicted. Related results are obtained with the fragments M(CO)₅ (M = Mo, W) (See ESI). Furthermore, additional peaks related to the perylene system are found ca. 262–266 nm in all the complexes, for example at 264 and 262 nm for gold derivatives **5a** and **5b**, comparable to those found in isocyanide free ligand at 263 and 260 nm for PMI-N≡C and Per-N≡C, respectively. Other absorptions corresponding to interligand charge transfer (LLCT) have been found, in accordance with the analysis of the involved orbitals. The analysis of the bands shows the different behavior of both terminal ligands, which indicates that CO acts as an acceptor whereas C₆F₅ acts as donor group. In general, the calculations predict, an increased intensity, compared to the free ligand, for the bands associated to the perylene system in the complexes. This is also in agreement with the experimental values (Table 2).

As shown in Fig. 4, the HOMOs and LUMOs of **5a,b** and **9a,b** are basically located on the perylene fragment and have similar contours to those calculated for the isocyanides. There is some contribution of the metal center orbitals to the HOMOs only for complexes **9a,b**, and for **5a**, with some additional contribution of the C₆F₅ ligand. For **5b**, no mixing between the Per moiety and the AuC₆F₅ fragment was found, whether for the HOMO or for the LUMO. This observation indicates that the C≡N linker brings about very little electronic communication.

(b) Luminescence spectra. The luminescence data for the ligands and the metal complexes at room temperature in chloroform are listed in Table 4. Isocyanide ligands, isocyanide complexes, and carbene complexes exhibit strong fluorescence in solution and have a well defined vibronic fine structure (See Fig. 5). The similarity of the overall luminescence spectra of these complexes with the Per or PMI fragment in both the vibronic structure and the spectral position strongly suggests an intraligand π-π* transition where the ligand orbitals have been slightly modified by the presence of the metal. On the basis of the similar Stokes shifts between absorption and emission for the ligands and the complexes (lower than 1000 cm⁻¹) the luminescence observed can be assigned to π-π* fluorescence,⁴⁵ which was supported by the fact that the emission properties remain unchanged in the presence of air, and confirmed with the measurement of their emission lifetimes ~ 4 ns (see Table 4) and our TD-DFT calculation.

Both PMI-N≡C (**4a**) and Per-N≡C (**4b**) ligands exhibit emission spectra very similar to PMI and perylene, respectively (Figure 5A), but with significant energy shifts: a lower wavelength (blue shift) (420 cm⁻¹) relative to PMI for **4a** and a higher wavelength (red shift) (920 cm⁻¹) relative to Per for **4b**. The complexes with PMI-N≡C **5a**, **9a-12a** show strong luminescence and exhibit the characteristic fluorescence of PMI (Fig. 5B), similar resolution of the vibronic structure, and very small energy shifts (<150 cm⁻¹), except for the carbonyl derivatives with poorer vibronic resolution and notable red shift (1300–1600 cm⁻¹). Fig. 5C shows normalized emission spectra of Per-N≡C and their gold complexes **5b-12b**. As expected from the fact that the fluorescence spectrum should be a mirror image of the

absorption spectrum, the gold complexes **5b** and **6b** exhibit emission bands red shifted 1060 cm⁻¹ relative to perylene-isocyanide, differently from the blue shift observed for the PMI derivatives. The carbonyl complexes **9b-11b** show as well notable red shift (1100–1400 cm⁻¹).

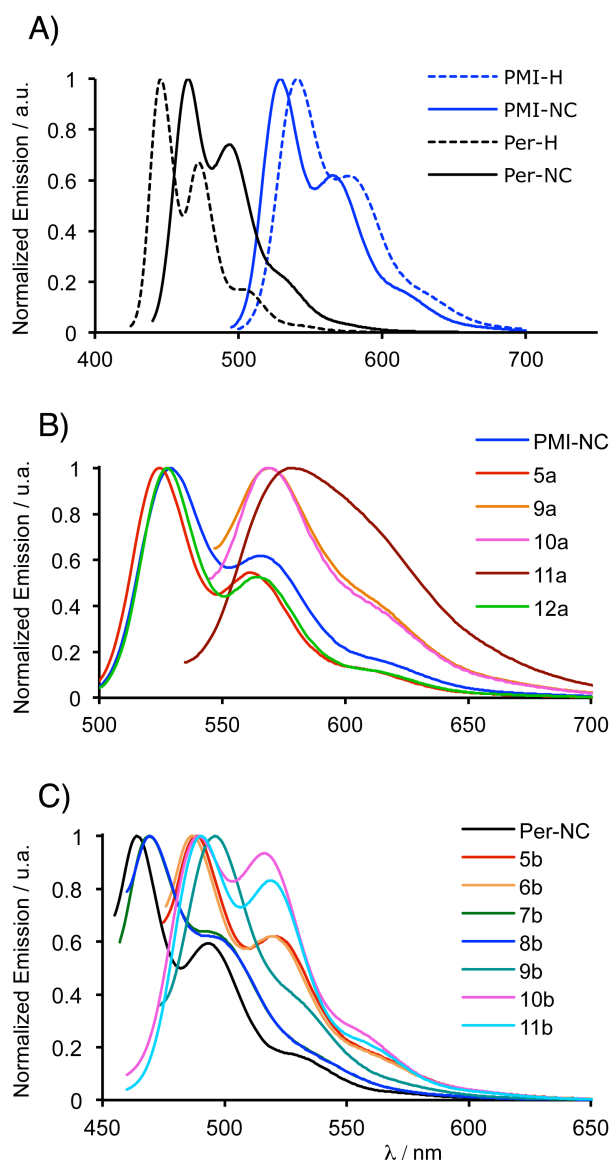


Fig. 5 Emission spectra recorded in CHCl₃ solution (approx. 10⁻⁵ M) at room temperature: A) PMI-N≡C (λ_{exc} = 476 nm) and Per-N≡C (λ_{exc} = 426 nm) ligands. B) PMI-N≡C and their complexes **5a**, **12a** (λ_{exc} = 477 nm) and **9a-11a** (λ_{exc} = 507 nm). C) Per-N≡C and their complexes **5b**, **6b** (λ_{exc} = 470 nm), **7b-11b** (λ_{exc} = 447 nm).

The effect of different solvents (acetonitrile, chloroform, tetrahydrofuran and toluene) on the emission spectra of **11b** was studied at room temperature (Fig. S4 in ESI). The nearly identical emission maxima (< 100 cm⁻¹) indicate that the fluorescence of the perylene derivative is hardly sensitive to the polarity of the solvents

Table 4 Emission and excitation in chloroform solution (10^{-5} M) at 298 K. ^a Determined in dichloromethane using Rhodamine B in ethanol ($\Phi_{\text{n}} = 0.70$) and using an excitation wavelength of 510 nm). ^b Determined in dichloromethane relative to perylene in ethanol ($\Phi_{\text{n}} = 0.92$) and using an excitation wavelength of 407 nm in CH_2Cl_2 .

Comp	$\lambda_{\text{ex}}/\text{nm}$	$\lambda_{\text{em}}/\text{nm}$	$\Phi_{\text{n}}^{\text{a}}$	τ/ns
4a	476, 506	529, 566	0.78	4.60
5a	477, 507	525, 561	0.77	4.19
9a	474, 504	569, 612sh	0.09	4.40
10a	478, 503	569, 612sh	0.06	4.39
11a	480, 504	578, 619sh	0.05	4.39
12a	477, 510	527, 563	0.80	3.57
4b	426, 452	464, 493	0.99 ^b	4.63
5b	444, 470	488, 520	0.88 ^b	4.25
6b	444, 470	488, 520	0.71 ^b	4.15
7b	423, 449	469, 492	0.69 ^b	3.67
8b	424, 449	469, 497	0.93 ^b	3.67
9b	405, 426, 453	496, 522sh	0.08 ^b	4.13
10b	445, 470	489, 517	0.44 ^b	1.52
11b	447, 472	490, 519	0.39 ^b	2.63

The shift produced by the carbene groups relative to perylene is lower than observed for the corresponding gold isocyanides complexes. Thus, the carbene complexes **7b** and **8b** are blue shifted (830 cm^{-1}) relative to the isocyanide complexes, and red shifted (1150 cm^{-1}) relative to perylene.

The emission quantum yields, Φ_{n} , measured in dichloromethane at room temperature, for the isocyanide ligands (0.78 for PMI-N≡C, and 0.99 for Per-N≡C) and their gold complexes (in the range 0.69 – 0.88) (Table 4) show that the perylenyl gold or palladium complexes reported here are highly fluorescent. An remarkable metal-depending effect is observed with the metal-carbonyl derivatives **9a–11a**. Thus, the coordination of the metal fragment causes notable singlet deactivation, somewhat metal sensitive (the emission quantum yields, Φ_{n} , is Cr (0.09) > Mo (0.06) > W (0.05)), but the fluorescence is not completely quenched. Similar behavior is found for the Per-N≡C carbonyl chromium complex **9b**, which exhibits similar low fluorescence quantum yield ($\Phi_{\text{n}} = 0.09$), although the molybdenum and tungsten complexes **10b–11b** are clearly more luminescent ($\Phi_{\text{n}} = 0.44$ for Mo, and 0.39 for W). It is not easy to assign this effect to a single cause.

Conclusions

The first perylene isocyanide complexes have been synthesized by attaching a $\text{AuC}_6\text{F}_4\text{X}$ ($\text{X} = \text{F}, \text{OBU}$) or $\text{M}(\text{CO})_5$ ($\text{M} = \text{Cr}, \text{Mo}, \text{W}$) fragment to 3-isocyanoperylene (Per-N≡C) or *N*-(2,5-di-*tert*-butylphenyl)-9-isocyano-perylene-3,4-dicarboximide (PMI-N≡C). The coordination of ML_n fragments to perylenyl isocyanides has a moderate quenching effect on the fluorescence, but the complexes are still highly fluorescent (in the range 70–90%), with the exception of the carbonyl derivatives where a lower quantum yield is observed. Theoretical calculations of the absorption spectra of the perylenyl isocyanide ligands $\text{C}\equiv\text{N-R}$ ($\text{R} = \text{PMI}, \text{Per}$) and the complexes $[\text{Au}(\text{C}_6\text{F}_5)(\text{CNR})]$ and $[\text{M}(\text{CO})_5(\text{CNR})]$ ($\text{M} = \text{Cr},$

Mo, W) indicate a very weak interaction of the metal with the π -system of the R fragment, which explains the retention of high quantum yields. Similar red shifts have been found in metal carbonyl complexes for both isocyanides, but for the fragment $\text{Au}(\text{C}_6\text{F}_5)$ or for the free isocyanide the bathochromic shift is bigger for the Per derivatives than for the PMI derivatives. Fluorescent metal complexes obtained with these luminescent markers can be of interest in a number of fields, for instance in biological studies.

Experimental section

Materials and general methods

All reactions were carried out under dry nitrogen. The solvents were purified according to standard procedures. Literature methods were used to prepare 3-aminoperylene, *N*-(2,5-di-*tert*-butylphenyl)-9-bromo-perylene-3,4-dicarboximide,⁴⁶ *N*-(2,5-di-*tert*-butylphenyl)-9-amino-perylene-3,4-dicarboximide,²⁹ *cis*-[Pd(C₆F₃Cl₂)₂(THF)₂].⁴⁷ C, H, N analyses were carried out on a Perkin-Elmer 2400 microanalyzer. IR spectra (cm^{-1}) were recorded on a Perkin-Elmer FT-1720X spectrometer. ¹H and ³¹P NMR spectra were recorded on Bruker AC 300 or Bruker 400 MHz spectrophotometers in CDCl_3 , with chemical shifts referred to TMS and 85% H_3PO_4 , respectively. UV-Vis absorption spectra were obtained on a Shimadzu UV-1603 spectrophotometer, in chloroform solution (1×10^{-5} M). Luminescence data were recorded on a Perkin-Elmer LS-luminescence spectrometer, in CHCl_3 (1×10^{-5} M) and in solid state measurements were made using finely pulverized KBr dispersions of the sample in 5 mm quartz tubes at room temperature. Luminescence quantum yields were obtained at room temperature using the optically dilute method ($A < 0.1$) in degassed dichloromethane (quantum yields standards were perylene in ethanol ($\Phi_{\text{n}} = 0.92$), and Rhodamine B in ethanol ($\Phi_{\text{n}} = 0.70$), using an excitation wavelength of 407 and 510 nm, respectively, in dichloromethane).^{48,49} The emission lifetime measurements were carried out with a Lifespec-red picosecond fluorescence lifetime spectrometer from Edinburgh Instruments. As excitation sources two diode lasers, with 405 and 470 nm nominal wavelengths were used. The first wavelength (405 nm) has a pulse width of 88.5 picoseconds, with a typical average power of 0.40 mW. The second wavelength (470 nm) has a pulse width of 97.2 picoseconds, and its typical average power is 0.15 mW. The pulse period is 1 μs and the pulse repetition frequency is 10 MHz. The monochromator slit is 2 nm. The instrument response measure at the HWHM (half with a high maximum) was below 350 picoseconds. The technique used is “Time Correlated Single Photon Counting” (TCSPC).

Computational details

Unrestricted calculations were carried out using the Gaussian09 package.⁵⁰ The hybrid density function method B3LYP was applied.⁵¹ Effective core potentials (ECP) were used to represent the innermost electrons of the transition atoms (Cr, Mo, W and Au) and the basis set of valence double- z quality for associated with the pseudopotentials LANL2DZ.⁵² The basis set for the main group elements was 6-31G* (Br, P, C, N, F and H).⁵³ Solvent effects of chloroform were taken into account by PCM calculations,⁵⁴ keeping the geometry optimized for gas phase (single-point calculations). Excited states and absorption spectra were obtained from the time-depending algorithm implemented in Gaussian09.⁵⁵

Synthesis of 4a. The procedure described by Ugi was followed,³⁰ but using triphosgene as dehydrating agent. A flask provided with a Dean-Stark apparatus was charged with de *N*-(2,5-ditercbutylphenyl)-9-amino-perylene-3,4-dicarboximide (0.600 g,

0.66 mmol) in 60 mL of toluene. Formic acid (1.5 mL) was added and the resulting suspension was refluxed for 1 h and then cooled to room temperature, the solvent was removed under vacuum and the crude product was washed with hexane (2 x 15 mL) and *N*-(2,5-ditercbutylphenyl)-9-formamide-perylene-3,4-dicarboximide was obtained (0.550 g, 94%). The violet crude product was sufficiently pure for use in the next reaction.

To a suspension of the formamide (0.500, 0.90 mmol) and triethylamine (0.37 mL, 2.71 mmol) in 100 mL of CH₂Cl₂ was added dropwise a solution of triphosgene (0.092 g, 0.31 mmol) in 10 mL of CH₂Cl₂. The mixture was stirred for 5 h and the solvent was removed on a rotary evaporator. The resulting residue was chromatographed (silica gel, CH₂Cl₂ as eluent) and the solvent was evaporated to obtain the product as a red solid. Yield 0.333 g (69%). Rf (silicagel, CH₂Cl₂/hexano 3:1): 0.45. ¹H RMN (300 MHz, CDCl₃): δ 8.69 (m, 2H), 8.56 (d, *J* = 7.5 Hz, 1H), 8.51 (d, *J* = 7.9 Hz, 1H), 8.46 (d, *J* = 8.3 Hz, 1H), 8.41 (d, *J* = 8.3 Hz, 1H), 8.26 (d, *J* = 8.3 Hz, 1H), 7.83 (t, *J* = 7.9 Hz, 1H), 7.73 (d, *J* = 8.2 Hz, 1H), 7.61 (d, *J* = 8.3 Hz, 1H), 7.47 (dd, *J* = 8.8 Hz, *J* = 2.2 Hz, 1H), 7.04 (d, *J* = 2.2 Hz, 1H), 1.34 (s, 9H, ¹Bu), 1.31 (s, 9H, ¹Bu). IR (KBr, cm⁻¹): 2112 ν(C≡N), 1707, 1669 ν(C=O). MS *m/z*: 534.

Synthesis of 4b. A flask provided with a Dean-Stark apparatus was charged with 3-aminoperylene (0.700 g, 2.62 mmol) in 60 mL of toluene. Formic acid (1.5 mL) was added and the resulting suspension was refluxed for 1 h and then cooled to room temperature, the solvent was removed under vacuum and the crude product was washed with diethyl ether (2 x 10 mL) and *N*-(perylene-3-yl)formamide was obtained (0.650 g, 93%). The crude product was sufficiently pure for use in the next reaction.

To a suspension of the formamide (0.325g, 1.10 mmol) and triethylamine (0.46 mL, 3.3 mmol) in 20 mL of CH₂Cl₂ was added dropwise a solution of triphosgene (0.11g, 0.37 mmol) in 10 mL of CH₂Cl₂. The mixture was stirred for 48 h and the solvent was removed on a rotary evaporator. The resulting residue was chromatographed (silica gel, CH₂Cl₂:hexane 3:1 as eluent) and the solvent was evaporated to obtain the product as a brown solid. Yield 0.160 g (53%). Rf (silicagel, CH₂Cl₂/hexano 3:1): 0.7. ¹H RMN (400 MHz, CDCl₃): δ 8.23 (d, *J* = 6.9 Hz, 1H), 8.19 (d, *J* = 6.9 Hz, 1H), 8.13 (d, *J* = 6.9 Hz, 1H), 8.03 (d, *J* = 8.1 Hz, 1H), 7.96 (d, *J* = 8.3 Hz, 1H), 7.73 (t, *J* = 7.8 Hz, 2H), 7.66 – 7.58 (m, 1H), 7.54 – 7.42 (m, 3H). IR (KBr, cm⁻¹): 2120 ν(C≡N). MS *m/z*: 277.

Synthesis of 5a. To a solution of [AuC₆F₅(tht)] (0.021 g, 0.046 mmol) in dichloromethane (15 mL) was added **4a** (0.025 g, 0.046 mmol). After the mixture had been stirred for 1 h, the resulting precipitate was filtrated and washed with diethyl ether (2x15 mL) and vacuum dried. Yield 35 mg (85%). C₄₃H₃₀F₅N₂O₂Au: calcd. C, 57.47; H, 3.36; N, 3.12. Found: C, 56.87; H, 3.50; N, 2.75. IR (KBr, cm⁻¹): 2202 ν(C≡N); 1708, 1665 ν(C=O).

Synthesis of 5b. The method was the same as that above but with the use of Per-N≡C (**4b**). Yield 40 mg (86%). Anal. Calcd. C₂₇H₁₁AuF₅N: C, 50.57; H, 1.73; N, 2.18. Found: C, 50.25; H, 1.63; N, 2.27. ¹H RMN (300 MHz, THF-d₈): δ 8.52 (d, *J* = 7.4 Hz, 1H), 8.43 (t, *J* = 7.4, 3H), 8.05-8.01 (m, 2H), 7.90-7.78 (m, 3H) 7.61-7.55 (m, 2H). ¹⁹F RMN (THF-d₈): δ = -111.3 (m, 2F^{ortho}), -163.1 (m, 1F^{para}, 2F^{meta}). IR (KBr, cm⁻¹): 2201 ν(C≡N).

Synthesis of 6b. To a solution of HC₆F₄-OEt-*p* (0.080 g, 0.41 mmol) in THF (20 mL) was added a solution of BuLi (1.6 M in hexane, 270 mL, 0.43 mmol) at -78 °C under an atmosphere of nitrogen. After the solution was stirred for 1 h at -50 °C, solid [AuCl(tht)] (0.131 g, 0.41 mmol) was added at -78 °C, and the reaction mixture was slowly brought to 10 °C (3 h). Then, a few drops of water were added, and the solution was filtered through anhydrous Na₂SO₄ and **5a** (0.114 g, 0.373 mmol) was added to the solution obtained. After stirring for 1 h, the solution was filtered

through Kieselguhr and silica gel. The solution was concentrated to ca. 5 mL and complex **6b** was precipitated by addition of hexane (30 mL) as an orange solid. Yield 0.171 g, 60%. Anal. Calcd for C₃₁H₂₀AuF₄NO: C, 53.54; H, 2.90; N, 2.01. Found: C, 53.00; H, 2.61; N, 2.55. ¹H RMN (300 MHz, THF-d₈): δ 8.50 (d, *J* = 7.2 Hz, 1H), 8.44 – 8.37 (m, 3H), 8.00 (dd, *J* = 8.4 Hz, 2.4 Hz, 2H), 7.89 – 7.76 (m, 3H), 7.58 (t, *J* = 7.3 Hz, 2H), 4.15 (t, *J* = 6.6 Hz, 2H, -OCH₂(CH₂)₂CH₃), 1.56 – 1.48 (m, 4H, -OCH₂(CH₂)₂CH₃), 0.97 (t, *J* = 7.8 Hz, 3H, -OCH₂(CH₂)₂CH₃). ¹⁹F RMN (THF-d₈): *d* -117.4 (m, 2F^{ortho}), -157.4 (m, 2F^{meta}). IR (KBr, cm⁻¹): 2202 ν(C≡N).

Synthesis of 7b. Diethylamine (30 μL 0.29 mmol) was added to a solution of **5b** (0.089 g, 0.14 mmol) in dichloromethane (45 mL). After 15 min of stirring at room temperature, the IR of the solution did not show CN absorption. Then the solution was evaporated to ca. 5 mL under reduced pressure. Addition of diethyl ether afforded an orange solid, which was filtered of, washed with diethyl ether (2 x 5 mL) and vacuum dried. Yield 85 mg, 85%. Anal. Calcd. for C₃₁H₂₂AuF₅N₂: C, 52.11; H, 3.10; N, 3.92. Found: C, 51.82; H, 2.88; N, 3.57. ¹H RMN (300 MHz, THF-d₈): δ 9.28 (s, 1H, NH), 8.40 – 8.25 (m, 4H), 7.90 – 7.80 (m, 2H), 7.71 (d, *J* = 7.8 Hz, 2H), 7.60 – 7.40 (m, 3H), 4.17 (q, *J* = 6.8 Hz, 2H, NCH₂), 3.70 (q, *J* = 7.3 Hz, 2H, NCH₂), 1.46 (m, 6H, N(CH₂Me)₂). ¹⁹F RMN (THF-d₈): *d* -115.3 (m, 2F^{ortho}), -162.7 (t, *J* = 20.3 Hz, 1F^{para}), -162.4 (m, 2F^{meta}). IR (KBr, cm⁻¹): 3353 ν(N-H), 1543 ν(C=N).

Synthesis of 8b. Diethylamine (18 μL 0.172 mmol) was added to a solution of **6b** (0.040 g, 0.057 mmol) in dichloromethane (30 mL). After 15 min of stirring at room temperature, the solution was filtered through silica gel. Addition of hexane afforded which was filtered of, washed with diethyl ether (2 x 5 mL) and vacuum dried. Yield 31 mg, 70%. Anal. Calcd. for C₃₅H₃₁AuF₄N₂O: C, 54.69; H, 4.07; N, 3.64. Found: C, 54.94; H, 3.89; N, 3.92. ¹H RMN (300 MHz, CDCl₃): δ 8.30 – 8.15 (m, 4H), 8.11 (d, *J* = 8.3 Hz, 1H), 7.75 – 7.68 (m, 3H), 7.64 (d, *J* = 7.9 Hz, 1H), 7.60 – 7.45 (m, 3H), 4.20 (q, *J* = 7.1 Hz, 2H, NCH₂), 4.03 (t, *J* = 6.6 Hz, OCH₂), 3.60 (q, *J* = 7.3 Hz, 2H, NCH₂), 1.70 – 1.30 (m, 12H), 0.89 (t, *J* = 7.5 Hz, 3H, Me). ¹⁹F RMN (THF-d₈): δ -118.2 (m, 2 F^{ortho}), -158.1 (m, 2F^{meta}). IR (KBr, cm⁻¹): 3354 ν(N-H), 1543 ν(C=N).

Synthesis of 9a. A solution of trimethylamine N-oxide (4 mg, 0.046 mmol) in MeCN (10 mL) was added to a suspension of [Cr(CO)₆] (12 mg, 0.046 mmol) in MeCN (20 mL) under nitrogen. The yellow solution formed was stirred for 6 h and the solvent was removed under vacuum. The yellow residue was solved in CH₂Cl₂ (20 mL) and a solution of **4a** (25 mg, 0.046 mmol) in CH₂Cl₂ (10 mL) was added dropwise. After stirring for 20 h the solvent was removed under vacuum to give the product as a red solid which was washed with diethyl ether (2 x 10 mL). Yield 23 mg, 66%). Anal. Calcd. for C₄₂H₃₀CrN₂O₇: C, 69.42; H, 4.16; N, 3.85. Found: C, 69.24; H, 3.89; N, 3.62. ¹H RMN (500 MHz, CDCl₃): δ 8.70 (m, 2H), 8.60 (d, *J* = 8.1 Hz, 1H), 8.53 (d, *J* = 8.1 Hz, 1H), 8.48 (d, *J* = 8.1 Hz, 1H), 8.44 (d, *J* = 8.2 Hz, 1H), 8.13 (d, *J* = 8.3 Hz, 1H), 7.87 (t, *J* = 8.0 Hz, 1H), 7.69 (d, *J* = 8.0 Hz, 1H), 7.59 (d, *J* = 8.6 Hz, 1H), 7.46 (dd, *J* = 8.6 Hz, *J* = 2.2 Hz, 1H), 7.01 (d, *J* = 2.2 Hz, 1H), 1.33 (s, 9H, ¹Bu), 1.29 (s, 9H, ¹Bu). IR (KBr, cm⁻¹): 2127 ν(C≡N); 2046, 2000, 1960 ν(C=O), 1707, 1664 ν(C=O).

Synthesis of 9b. The method was the same as that above but with the use of Per-N≡C (**4b**). Yield 23 mg, 74%. Anal. Calcd. for C₂₆H₁₁CrNO₅: C, 66.53; H, 2.36; N, 2.98. Found: C, 66.29; H, 2.31; N, 2.78. ¹H RMN (500 MHz, CDCl₃): δ 8.32 (d, *J* = 7.6 Hz, 1H), 8.26 (d, *J* = 7.5 Hz, 1H), 8.21 (d, *J* = 7.6 Hz, 1H), 8.14 (d, *J* = 8.1 Hz, 1H), 7.87 (d, *J* = 8.3 Hz, 1H), 7.77 (t, *J* = 7.7 Hz, 2H), 7.71 (d, *J* = 7.9 Hz, 1H), 7.54 (m, 3H). IR (cm⁻¹): 2134 ν(C≡N); 2055, 2005, 1936 ν(C=O).

Synthesis of 10a and 11a. To a mixture of [M(CO)₆] (M = Mo, W) (0.046 mmol) and PMI-N≡C (**4a**) (25 mg, 0.046 mmol) in THF

(30 mL) was added dropwise a solution of trimethylamine N-oxide (4 mg, 0.046 mmol) in 10 mL of THF under nitrogen. After stirring overnight, the solvent was evaporated and the resulting residue was washed with hexane (2 × 10 mL).

M = Mo, Yield 17 mg, 55%. Anal. Calcd. for C₄₂H₃₀N₂O₇Mo: C, 65.46; H, 3.92; N, 3.64. Found: C, 65.29; H, 3.70; N, 3.35. ¹H RMN (500 MHz, CDCl₃): δ 8.70 (m, 2H), 8.61 (d, *J* = 7.7 Hz, 1H), 8.54 (d, *J* = 8.1 Hz, 1H), 8.50 (d, *J* = 8.1 Hz, 1H), 8.46 (d, *J* = 8.3 Hz, 1H), 8.13 (d, *J* = 8.3 Hz, 1H), 7.89 (t, *J* = 8.0 Hz, 1H), 7.73 (d, *J* = 8.1 Hz, 1H), 7.59 (d, *J* = 8.6 Hz, 1H), 7.46 (dd, *J* = 8.6 Hz, *J* = 2.3 Hz, 1H), 7.02 (d, *J* = 2.2 Hz, 1H), 1.33 (s, 9H, ^tBu), 1.29 (s, 9H, ^tBu). IR (KBr, cm⁻¹): 2126 ν(C≡N), 2049, 2000, 1954 ν(C=O), 1707, 1664 ν(C=O).

M = W, Yield 20 mg, 52%. Anal. Calcd. for C₄₂H₃₀N₂O₇W: C, 58.76; H, 3.52; N, 3.26. Found: C, 58.37; H, 3.50; N, 3.05. ¹H RMN (400 MHz, CDCl₃): δ 8.71 (m, 2H), 8.61 (d, *J* = 7.8 Hz, 1H), 8.54 (d, *J* = 8.1 Hz, 1H), 8.48 (d, *J* = 8.1 Hz, 1H), 8.45 (d, *J* = 8.3 Hz, 1H), 8.12 (d, *J* = 8.1 Hz, 1H), 7.89 (t, *J* = 8.1 Hz, 1H), 7.73 (d, *J* = 8.3 Hz, 1H), 7.60 (d, *J* = 8.5 Hz, 1H), 7.47 (dd, *J* = 8.5 Hz, *J* = 2.2 Hz, 1H), 7.01 (d, *J* = 2.1 Hz, 1H), 1.33 (s, 9H, ^tBu), 1.29 (s, 9H, ^tBu). IR (KBr, cm⁻¹): 2128 ν(C≡N), 2044, 2000, 1954 ν(C=O), 1707, 1664 ν(C=O).

Synthesis of 10b and 11b. The method was the same as that above but with the use of Per-N≡C (**4b**).

M = Mo Yield 32 mg, 64%. Anal. Calcd. for C₂₆H₁₁MoNO₅: C, 60.84; H, 2.16; N, 2.73. Found: C, 60.53; H, 2.41; N, 2.63. ¹H RMN (400 MHz, CDCl₃): δ = 8.33 (d, *J* = 7.6 Hz, 1H), 8.27 (d, *J* = 7.5 Hz, 1H), 8.22 (d, *J* = 7.6 Hz, 1H), 8.15 (d, *J* = 8.2 Hz, 1H), 7.87 (d, *J* = 8.3 Hz, 1H), 7.77 (t, *J* = 7.6 Hz, 2H), 7.72 (t, *J* = 7.9 Hz, 1H), 7.60 – 7.50 (m, 3H). IR (cm⁻¹): 2131 ν(C≡N); 2055, 1933 ν(C=O).

M = W Yield 47 mg, 85%. Anal. Calcd. for C₂₆H₁₁WNO₅: C, 51.94; H, 1.84; N, 2.33. Found: C, 51.89; H, 2.05; N, 2.37. ¹H NMR (500 MHz, CDCl₃) δ = 8.31 (d, *J* = 7.5 Hz, 1H), 8.26 (d, *J* = 7.5 Hz, 1H), 8.21 (d, *J* = 7.5 Hz, 1H), 8.13 (d, *J* = 8.1 Hz, 1H), 7.84 (d, *J* = 8.2 Hz, 1H), 7.77 (t, *J* = 8.4 Hz, 2H), 7.71 (t, *J* = 7.9 Hz, 1H), 7.56 – 7.51 (m, 3H). IR (cm⁻¹): 2136 ν(C≡N); 2055, 2005, 1937 ν(C=O).

Synthesis of 12a and 12b. To a solution of *cis*-Pd(C₆F₃Cl₂)₂(THF)₂ (25 mg, 0.038 mmol) in CH₂Cl₂ was added the corresponding isocyanide CNR (0.076 mmol) and the mixture was stirred 0.5 h. The resulting precipitate was filtered and washed with diethyl ether (2 × 10 mL).

12a: Yield 44 mg, 74%. Anal. Calcd. for C₈₆H₆₀Cl₄F₆N₄O₄Pd: C, 65.56; H, 3.84; N, 3.56. Found: C, 65.40; H, 3.67; N, 3.49. ¹H RMN (300 MHz, THF-*d*₆): δ 8.80–8.60 (m, 10H), 8.04 (d, *J* = 7.2 Hz, 2H), 7.98 (d, *J* = 7.8 Hz, 2H), 7.83 (t, *J* = 7.8 Hz, 2H), 7.55 (d, *J* = 8.5 Hz, 2H), 7.42 (dd, *J* = 1.8 Hz, *J* = 8.4 Hz, 2H), 7.13 (d, *J* = 2.4 Hz, 2H), 1.31 (s, 18 H, 2^tBu), 1.26 (s, 18 H, 2^tBu). ¹⁹F RMN (THF-*d*₆) -87.6 (s, 2 F_{ortho}), -118.0 (s, 1 F_{para}). IR (KBr, cm⁻¹): 2171 ν(C≡N), 1709, 1669 ν(C=O).

12b: Yield 34 mg, 84%. Anal. Calcd. for C₅₄H₂₂Cl₄F₆N₂Pd: C, 61.13; H, 2.09; N, 2.64. Found: C, 60.80; H, 1.87; N, 2.59. IR (KBr, cm⁻¹): 2176 ν(C≡N).

X-ray Crystal Structure Analysis

Single crystals of **7b** and **8b** suitable for X-ray diffraction studies were obtained from slow diffusion of hexane into a dichloromethane solution of the crude products at -20 °C, under nitrogen. Crystals were mounted in glass fibers, and diffraction measurements were made using a Bruker AXS SMART 1000 CCD diffractometer, using φ and ω scans, Mo-Kα radiation (λ = 0.71073 Å), graphite monochromator, and *T* = 298 K. Raw frame data were integrated with SAINT⁵⁶ program. Structures were solved by direct methods with SHELXTL.⁵⁷ Semi-empirical absorption correction was made with SADABS.⁵⁸ All non-hydrogen atoms were refined

anisotropically. Hydrogen atoms were set in calculated positions and refined as riding atoms, with a common thermal parameter. All calculations were made with SHELXTL. For **8b** the butyl group was found to be affected by an incipient disorder, which was not possible to be satisfactorily modeled. Therefore the butyl was refined as a rigid group. Crystallographic data (excluding structure factors) for the structures reported in this paper have been deposited with the Cambridge Crystallographic Data Centre as Supplementary publications with the following deposition numbers: CCDC 970735 and 970736 for complexes **7b** and **8b**, respectively. These data can be obtained free of charge from The Cambridge Crystallographic Data Centre via www.ccdc.cam.ac.uk/data_request/cif rigid group. Crystallographic data (excluding structure factors) for the structures reported in this paper have been deposited with the Cambridge Crystallographic Data Centre as Supplementary publications with the following deposition numbers: CCDC 970735 and 970736 for complexes **7b** and **8b**, respectively. These data can be obtained free of charge from The Cambridge Crystallographic Data Centre via www.ccdc.cam.ac.uk/data_request/cif.

Table 5 Crystal and structure refinement data for **7b** and **8b**

	7b	8b
Empirical formula	C ₃₁ H ₂₂ AuF ₅ N ₂	C ₃₅ H ₃₁ AuF ₄ N ₂ O
Formula weight	714.47	768.58
Temperature (K)	298(2)	298(2)
Wavelength (Å)	0.71073	0.71073
Crystal system	Triclinic	Monoclinic
Space group	P-1	P2(1)/c
<i>a</i> (Å)	7.703(3)	12.312(3)
<i>b</i> (Å)	11.939(5)	18.978(4)
<i>c</i> (Å)	15.079(6)	13.736(3)
α (deg)	71.471(7)	90
β (deg)	86.857(7)	106.512(4)
γ (deg)	76.382(7)	90
<i>V</i> (Å ³)	1277.6(9)	3077.2(12)
<i>Z</i>	2	4
<i>D</i> _{calc} (g cm ⁻³)	1.857	1.659
Absorpt. coefficient (mm ⁻¹)	5.818	4.835
<i>F</i> (000)	692	1512
Crystal size (mm)	0.33 × 0.12 × 0.05	0.18 × 0.15 × 0.05
Theta range for data collection	1.42 a 26.81	1.88 a 26.44
Reflections collected	11396	26339
Independent reflections	5365	6310
Absorption correction	SADABS	SADABS
Max. and min. transmission factor	1.0000 and 0.540333	1.0000 and 0.744209
Data/restraints/parameters	5365 / 0 / 354	6310 / 0 / 391
Goodness-of-fit on F ²	1.035	1.016
<i>R</i> ₁ [<i>I</i> > 2σ(<i>I</i>)]	0.0323	0.0494
<i>wR</i> ₂ (all data)	0.0823	0.1534

Acknowledgements

We thank the Spanish Ministerio de Economía y Competitividad (CTQ2011-2513 and CTQ2011-23862-C02); the Junta de Castilla y León (Project VA302U13); and the Generalitat de Catalunya (grant 2009SGR-1459) for financial support. Computing resources at the Centre de Supercomputació de Catalunya (CESCA) were used through a grant of Fundació Catalana per a la Recerca (FCR).

Notes and references

^a IU CINQUIMA/Química Inorgánica, Facultad de Ciencias, Universidad de Valladolid, 47071 Valladolid (Spain).

^b Departament de Química Inorgànica, Universitat de Barcelona, Martí i Franquès 1-11, E-08028 Barcelona, (Spain).

† Electronic Supplementary Information (ESI) available: Absorption spectra; schematic representation of main expected transition in the absorption spectra of PMIH, and perylene; calculated absorption spectra parameters for R-X (R = PMI, Per; X = H, NC), [Au(CN-R)(C₆F₅)] (R = PMI, Per), and [M(CO)₅(CNR)] (M = Cr, Mo, W; R = PMI, Per), in gas phase and chloroform solution; emission spectra of **11b** in different solvents at room temperature. CCDC reference numbers 970735 and 970736 For ESI and crystallographic data in CIF or other electronic format see DOI: 10.1039/b000000x/

- 1 F. Würthner, *Chem. Commun.* 2004, 1564.
- 2 H. Langhals, *Helv. Chim. Acta* 2005, **88**, 1309.
- 3 Zollinger, *Color Chemistry*, Wiley-VCH, Weinheim, 3rd ed, 2003.
- 4 (a) C. Li, H. Wonneberger, *Adv Mater.* 2012, **24**, 613. (b) E. Kozma, M. Catellani, *Dyes and Pigments*, 2013, **98**, 160.
- 5 M. R. Wasielewski, *J. Org. Chem.* 2006, **71**, 5051.
- 6 T. Weil, T. Vosch, J. Hofkens, K. Peneva and K. Müllen, *Angew. Chem., Int. Ed.* 2010, **49**, 9068.
- 7 X. Zhan, A. Facchetti, S. Barlow, T. J. Marks, M. A. Ratner, M. R. Wasielewski and S. R. Marder, *Adv. Mater.* 2011, **23**, 268.
- 8 C. Huang, S. Barlow and S. R. Marder, *J. Org. Chem.* 2011, **76**, 2386.
- 9 (a) F. Würthner, C. Thalacker, S. Diele and C. Tschierske, *Chem.–Eur. J* 2001, **7**, 2245. (b) Z. Chen, U. Baumeister, C. Tschierske and F. Würthner, *F. Chem.–Eur. J* 2007, **13**, 450. (c) Z. Chen, V. Stepanenko, V. Dehm, P. Prins, L. D. A. Siebbeles, J. Seibt, P. Marquetand, V. Engel and F. Würthner, *Chem.–Eur. J.* 2007, **13**, 2245.
- 10 F. Würthner, T. E. Kaiser and C. R. Saha-Möller, *Angew. Chem., Int. Ed.* 2011, **50**, 3376.
- 11 F. Castellano, *Dalton Trans.* 2012, **41**, 8493 and references cited therein.
- 12 S. Lentijo, J. A. Miguel and P. Espinet, *Inorg. Chem.* 2010, **49**, 9169.
- 13 H. Yersin and J. Strasser, *Coord. Chem. Rev.* 2000, **208**, 331.
- 14 A. K. Chandra, N. J. Turro, A. L. Jr. Lyons and P. Stone, *J. Am. Chem. Soc.* 1978, **100**, 4964.
- 15 H. Weissman, E. Shirman, T. Ben-Moshe, R. Cohen, G. Leitus, L. J. W. Shimon and B. Rybtchinski, *Inorg. Chem.* 2007, **46**, 4790.
- 16 (a) S. Lentijo, J. A. Miguel and P. Espinet, *Organometallics* 2011, **30**, 1059. (b) S. Lentijo, J. A. Miguel and P. Espinet, *Dalton Trans.* 2011, **40**, 7602.
- 17 G. Vilaca, K. Barathieu, B. Jousseume, T. Toupance and H. Allouchi, *Organometallics* 2003, **22**, 4584.
- 18 S. Lentijo, G. Aullón, J. A. Miguel and P. Espinet, *Dalton Trans.* 2013, **42**, 6353.
- 19 (a) F. Würthner and A. Sautter, *Chem. Commun.* 2000, 445. (b) F. Würthner, A. Sautter, D. Schmid and P. J. A. Weber, *Chem. Eur. J.* 2001, **7**, 894.
- 20 (a) R. Dobrawa and F. Würthner, *Chem. Commun.* 2002, 1878. (b) R. Dobrawa, M. Lysetska, P. Ballester, M. Grüne and F. Würthner, *Macromolecules* 2005, **38**, 1315.
- 21 (a) E. O. Danilov, A. A. Rachford, S. Goeb and F. N. Castellano, *J. Phys. Chem.*, 2009, **113**, 5763. (b) A. A. Rachford, S. Goeb, R. Ziessel and F. N. Castellano, *Inorg. Chem.*, 2008, **47**, 4348.
- 22 A. Sautter, D. G. Schmid, J. Günter and F. Würthner, *J. Am. Chem. Soc.* 2001, **123**, 5424.
- 23 K. Qvortrup, A. D. Bond, A. Nielsen, C. J. Mckenzie, K. Kilsa and M. B. Nielsen, *Chem. Commun.* 2008, 1986.
- 24 R. Benavente, P. Espinet, S. Lentijo, J. M. Martín-Alvarez, J. A. Miguel and M. P. Rodríguez-Medina, *Eur. J. Inorg. Chem.* 2009, 5399.
- 25 S. Coco, C. Cordovilla, P. Espinet, J. M. Martín-Alvarez and P. Muñoz, *Inorg. Chem.* 2006, **45**, 10180.
- 26 (a) C. Bartolomé, M. Carrasco-Rando, S. Coco, C. Cordovilla, J. M. Martín-Alvarez and P. Espinet, *Inorg. Chem.* 2008, **47**, 1616. (b) C. Bartolomé, M. Carrasco-Rando, S. Coco, C. Cordovilla, P. Espinet and J. M. Martín-Alvarez, *Dalton Trans.* 2007, 5339.
- 27 (a) R. Bayón, S. Coco and P. Espinet, *Chem. Eur. J.* 2005, **11**, 1079; *ibid. Chem. Eur. J.*, 2005, **11**, 3500. (corrigenda). (b) S. Coco, C. Cordovilla, C. Domínguez and P. Espinet, *Dalton Trans.* 2008, 6894.
- 28 (a) D. S. Grubisha, J. S. Rommel, T. M. Lane, W. T. Tysoe and D. W. Bennett, *Inorg. Chem.* 1992, **31**, 5022. (b) M. P. Guy, J. T. Jr. Guy and D. W. Bennett, *Organometallics* 1986, **5**, 1696. (c) M. P. Guy, J. L. Coffey, J. S. Rommel and D. W. Bennett, *Inorg. Chem.* 1988, **27**, 2942. (d) R. F. Johnston, *J. Coord. Chem.* 1994, **31**, 57.
- 29 S. Becker, A. Böhm and K. Müllen, *Chem. Eur. J.* 2000, **6**, 3984.
- 30 I. Ugi and R. Meyr, *Chem. Ber.* 1960, **93**, 239.
- 31 H. Eckert and B. Forster, *Angew. Chem., Int. Ed. Engl.* 1987, **26**, 894.
- 32 R. Bayón, S. Coco and P. Espinet, *Chem. Mater.* 2002, **14**, 3515.
- 33 (a) H. Chislmon and H. Clark, *Inorg. Chem.* 1971, **10**, 1711. (b) F. Bonati and G. Minghetti, *J. Organomet. Chem.* 1970, **24**, 251. (c) J. S. Miller and A. L. Bach, *Inorg. Chem.* 1972, **11**, 2069.
- 34 (a) R. A. Michelin, A. J. L. Pombeiro and M. F. C. Guedes da Silva, *Coord. Chem. Rev.* 2001, **218**, 75. (b) J. Vignolle, X. Cattoe and D. Bourissou, *Chem. Rev.* 2009, **109**, 3333.
- 35 (a) A. Busetto, A. Palazzi, B. Crociani, U. Belluco, E. Bradley, B. J. L. Kilby and R. L. Richards, *J. Chem. Soc., Dalton Trans.* 1972, 1800.
- 36 A. S. K. Hashmi, T. Hengst, C. Lothsch and F. Rominger, *Adv. Synth. Catal.* 2010, **352**, 1315.
- 37 (a) C. Bartolomé, Z. Ramiro, P. Pérez-Galán, C. Bour, M. Raducan, A. M. Echavarren and P. Espinet, *Inorg. Chem.* 2008, **47**, 11391. (b) C. Bartolomé, D. García-Cuadrado, Z. Ramiro and P. Espinet, *Inorg. Chem.* 2010, **47**, 9758.

- 38 (a) J. Vicente, M. T. Chicote, M. D. Abrisqueta and P. J. Jones, *Organometallics* 2000, **19**, 2629. (b) P. G. Jones, *J. Organomet. Chem.* 1988, **345**, 405.
- 39 (a) S. Coco, C. Cordovilla, C. Domínguez, B. Donnio, P. Espinet and D. Guillon, *Chem. Mater.* 2009, **21**, 3282. (b) P. Espinet, P. Gómez-Elipe and F. Villafañe, *J. Organomet. Chem.* 1992, **450**, 145.
- 40 M. O. Albers and N. Coville, *J. Chem. Soc. Dalton. Trans.* 1982, 1069.
- 41 T. Kaharu, T. Tanaka, M. Sawada and S. Takahashi, *J. Mater. Chem.* 1994, **4**, 859.
- 42 (a) B. Crociani, T. Boshi and V. Belluco, *Inorg. Chem.* 1970, **9**, 2021. (b) S. Coco, F. Diéz-Expósito, P. Espinet, C. Fernández-Mayordomo, J. M. Martín-Álvarez and M. Levelut, *Chem. Mater.* 1998, **10**, 3666.
- 43 L. Cuffè, R. D. A. Hudson, J. F. Gallagher, S. Jennings, C. J. McAdam, R. B. T. Connelly, A. R. Manning, B. H. Robinson and J. Simpson *Organometallics* 2005, **24**, 2051.
- 44 F. H. Allen, O. Kennard, D. G. Watson, L. Brammer, A. G. Orpen and R. Taylor, *J. Chem. Soc. Perkin Trans. II* 1987, *S1-S19*.
- 45 (a) J. R. Lakowicz, *Principles of Fluorescence Spectroscopy*, Plenum Press, New York, 1983. (b) G. G. Guilbault, *Fluorescence*, Second Edition, Marcel Dekker, Inc., New York, 1990.
- 46 (a) P. Schlichting, U. Rohr and K. Müllen, *Liebigs Ann/Recueil* 1997, 395. (b) K. Tomozaki, P. Thamyongkit, R. S. Loewe and J. S. Lindsey, *Tetrahedron* 2003, **59**, 1191.
- 47 P. Espinet, J. M. Martínez-Illarduya, C. Pérez-Briso, A. L. Casado and M. A. Alonso, *J. Organomet. Chem.* 1998, **551**, 9.
- 48 M. Montalti, A. Credi, L. Prodi and M. T. Gandolfini, *Handbook of Photochemistry*, 3rd ed.; CRC Pres LLC: Boca Raton, FL, 2005.
- 49 F. López-Arbeloa, P. Ruiz-Ojeda and I. López-Arbeloa, *J. Luminesc.* 1989, **44**, 105.
- 50 M. J. Frisch, et al. *Gaussian 09 (Revision B.1)*; Gaussian Inc, Wallingford, CT, 2010.
- 51 (a) A. D. Becke, *J. Chem. Phys.* **1993**, *98*, 5648. (b) C. Lee, W. Yang and R. G. Parr, *Phys. Rev. B* 1988, **37**, 785.
- 52 P. J. Hay and W. R. Wadt, *J. Chem. Phys.* 1985, **82**, 299.
- 53 (a) P. C. Hariharan and J. A. Pople, *Theoret. Chim. Acta* 1973, **28**, 213. (b) M. M. Francl, W. J. Pietro, W. J. Hehre, J. S. Binkley, M. S.; Gordon, D. J. DeFrees and J. A. Pople, *J. Chem. Phys.* 1982, **77**, 3654.
- 54 (a) J. Tomasi, and M. Persico, *Chem. Rev.* 1994, **94**, 2027. (b) C. Amovilla, V. Barone, R. Cammi, E. Cancès, M. Cossi, B. Mennucci, C. S. Pomelli and J. Tomasi, *Adv. Quantum Chem.* 1998, **32**, 227.
- 55 M. E. Casida, C. Jamorski, K. C. Casida and D. R. Salahub, *J. Chem. Phys.* 1998, **108**, 4439.
- 56 SAINT+. SAX area detector integration program. Version 6.02. Bruker AXS, Inc. Madison, WI, 1999.
- 57 G. M. Sheldrick, SHELXTL, An integrated system for solving, refining, and displaying crystal structures from diffraction data. Version 5.1. Bruker AXS, Inc. Madison, WI, 1998.
- 58 G. M. Sheldrick, *SADABS: A Program for Absorption Correction with the Siemens SMART System*, University of Göttingen, Germany, 1996.